Pergamon

Int. J. Heat Mass Transfer. Vol. 40, No. 1, pp. 159–167, 1997

0017–9310/97 $15.00 + 0.00

PII: S0017-9310(96)00084-1

Calculation of heat and moisture transfer in exposed building components

HARTWIG M. KÜNZEL and KURT KIESSL

Fraunhofer-Institut für Bauphysik, P.O. Box 1152, D-83601 Holzkirchen, Germany

(*Received* 29 *December* 1994 *and in final form* 22 *January* 1996)

Abstract—Understanding the hygrothermal behaviour of exposed building components is a first step in avoiding damage or undue heat loss from constructions. Since experimental investigations are rather expensive and of limited transferability, there is an urgent need for reliable heat and moisture transfer calculations applicable in building practice. Such a calculation method, which is based on physical evidence concerning vapour and liquid transport and new experimental results, is presented and the required material and climatic data are described. To validate the model the calculation results for the moisture behaviour of a facade exposed to driving rain and solar radiation are compared to well documented measurements. As a consequence of this comparison it appears that the described model provides accurate results despite simplifications concerning the material properties. Copyright © 1996 Elsevier Science Ltd.

1. INTRODUCTION

In civil engineering there is an increasing demand for calculative methods to assess the moisture behaviour of building components. Current tasks, such as preserving historical buildings or restoring, respectively insulating, existing constructions, are closely related to questions concerning present and future moisture conditions in a building structure. Due to expensive and time-consuming experimental investigations of the moisture behaviour of building components, calculative studies are becoming increasingly important. They are also useful for predicting the consequences of any constructive modifications or the effects of different climate conditions.

Considering the calculation techniques of the past, the most common approaches used the water content and the temperature as driving potentials for moisture transfer (e.g. [1, 2]). Since neither of these potentials is a physical driving force for vapour or liquid transport—the water content is not even a continuous potential—the calculation models based upon them appear to be outdated. More advanced models can be found for example in refs. [3–6]. The determination of the moisture dependent material properties, however, still remained complex and the application of the models was therefore restricted.

In order to arrive at a simpler, but still highly accurate calculation method a model based on new experimental results and physical evidence is presented, which requires less extensive measurements for the determination of the material data. The model and the basic assumptions are described in detail for two-dimensional calculations in ref. [7]. This paper will give a summary of the physical fundamentals and the one-dimensional application of this calculation method.

2. FUNDAMENTAL PRINCIPLES OF MOISTURE TRANSFER

Due to the limited scope of this paper, the fundamentals of heat transfer in porous media and the moisture influence on the heat capacity and transport are not addressed here. The same holds for the moisture transport in organic polymers and below freezing temperature. Both items can be found in ref. [7]. Here the principles of moisture retention, vapour and liquid flow in porous building materials will be investigated.

2.1. *Moisture retention*

Moisture in building materials can be present as vapour, water or ice, respectively, in some intermediate state as absorbed phase on the pore walls. Since it is in general not possible to differentiate between the different aggregate states, the water content is defined as the total moisture in a material. Since the water content of a material is generally in equilibrium with its local environment, a moisture retention function of the material is needed in order to describe this phenomena. Figure 1 shows such a storage function for a hygroscopic, capillary active material (e.g. a building stone). In the moisture range A this function is equal to the sorption isotherm of the material. Above *ca* 95% relative humidity the equilibrium water content is difficult to measure by sorption tests because of experimental uncertainties and the steep slope of the sorption isotherm. However, in this moisture range B, which extends from range A to the capillary saturation, there still exists an equilibrium between two different porous materials.

This can be explained by the suction stress in the capillary pores which depends on their radius. An equilibrium is reached when the suction stress in the two contacting materials is equal, i.e. the largest water

NOMENCLATURE

c	specific heat capacity [J kg^{-1} K^{-1}]	Greek symbols	
D_φ	liquid conductivity [kg m s^{-1}]	δ	vapour diffusion coefficient in air [kg m s^{-1} Pa^{-1}]
D_w	liquid diffusivity [m^2 s^{-1}]	δ_p	vapour permeability of the porous material [kg m s^{-1} Pa^{-1}]
g_v	vapour flux [kg m^{-2} s^{-1}]	λ	moisture dependent thermal conductivity [W m^{-1} K^{-1}]
g_w	liquid flux [kg m^{-2} s^{-1}]	μ	vapour diffusion resistance number
H_w	enthalpy of material moisture [J m^{-3}]	φ	relative humidity
h_v	specific heat of evaporation [J kg^{-1}]	ρ	material density [kg m^{-3}]
p	vapour pressure [Pa]	θ	temperature [°C].
p_{sat}	saturation vapour pressure [Pa]		
w	water content [kg m^{-3}]		
w_f	capillary (free) water saturation [kg m^{-3}].		

filled pores are of similar dimensions in both materials. When a material is in contact with liquid water the equilibrium water content is called capillary saturation with a suction stress close to zero. This does not mean that all the pores in the material are filled with water. In most building stones the capillary saturation is considerably smaller than their total porosity. In order to fill all pores a high pressure or vacuum has to be applied.

Between the capillary saturation and the maximum water saturation lies the moisture range C in Fig. 1. In this range there is no defined function between the water content and the suction stress, respectively, the relative humidity, which are the driving forces for moisture exchange under isothermal conditions. Therefore, above capillary saturation no clearly defined moisture equilibrium between two porous material samples should be expected. This can be tested by a simple experiment whose results are shown in Fig. 2. There the water content of pairs of building stone samples is plotted over a period of 40 days. A pair consists of two identical material slabs which are over one surface in close capillary contact with each other, while the other surfaces are sealed. Initially one sample of a pair has capillary saturation, while the other one has maximum saturation. Despite the high differences in water content there is almost no moisture exchange over the test period. The slight decrease in water content in the case of the lime silica brick samples is probably due to imperfect sealing.

The moisture retention function of a building material is thus composed of three parts: the sorption isotherm up to *ca* 95% relative humidity (moisture range A), the capillary moisture range (B) and the over saturated moisture range (C), where the water retention function is a vertical line at 100% r.h. The functional values in the moisture range B can be measured by a pressure plate apparatus [8], or approxi-

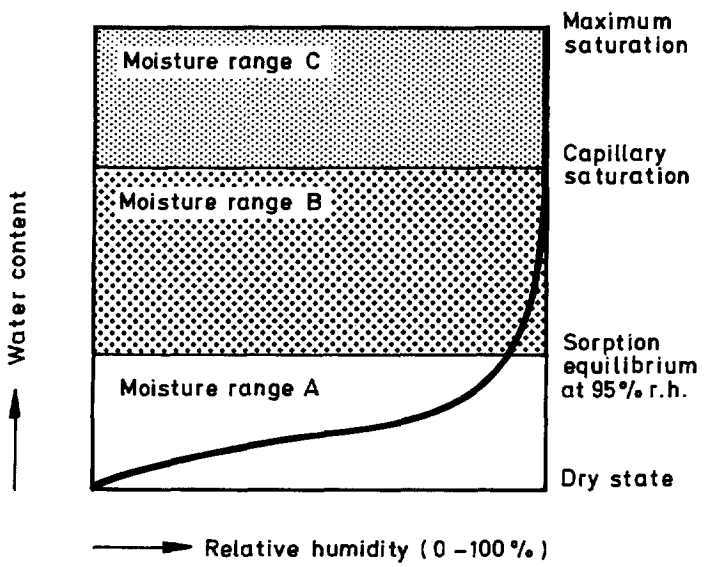

Fig. 1. Schematic representation of the water retention function of a hygroscopic, capillary active building material.

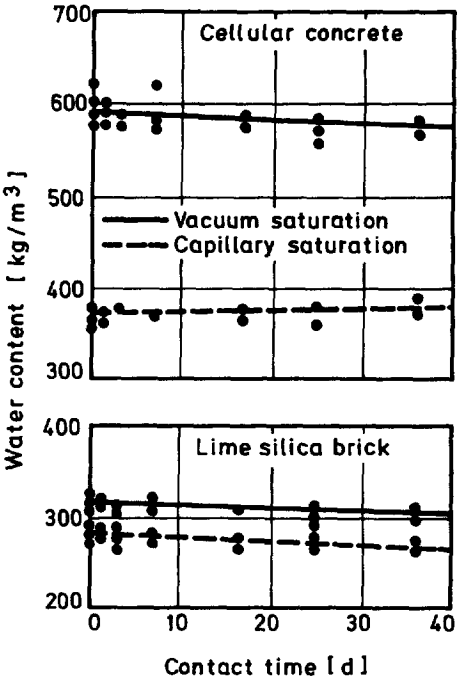

Fig. 2. Measured water content in sealed pairs of thin building stone slabs, one capillary saturated and the other one vacuum saturated after different periods of capillary contact.

mated from mercury intrusion porosimetry tests [3]. Since there is a well defined relationship between the capillary pressure (suction stress) and the relative humidity (Kelvin's law), the results from pressure plate measurements can be introduced directly into the water retention function. Figure 3 shows such a complete function for a natural sandstone (moisture range C is omitted because it contains no relevant information). It is in general unnecessary to differentiate between an absorption and desorption function, because the hysteresis is in most cases either negligible or insignificant for moisture transport calculations, as has been shown in ref. [4].

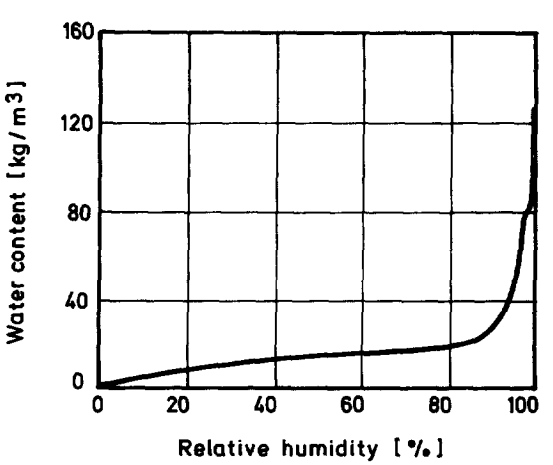

Fig. 3. Water retention function of Sander sandstone determined by sorption tests (up to 93% r.h.) and pressure plate measurements [14].

2.2. *Moisture transport*

If moisture convection either by air pressure or hydraulic pressure differences, respectively, gravity is excluded, the remaining mechanisms are vapour diffusion and liquid transport due to the differences in capillary suction stress. Both processes are in general largely independent of each other, as has been shown in ref. [9], because vapour diffusion is most important in large pores, whereas liquid transport takes place at pore surfaces, in crevices and small capillaries. The driving potential for the vapour diffusion is generally accepted to be the partial vapour pressure [10]. The driving force for water in the absorbed layer and in the small capillaries is capillary suction [5] or via Kelvin's law relative humidity.

In building components, both moisture potentials can be opposed to each other, which is explained by looking at a small capillary in a monolithic wall in Fig. 4. Under winter conditions the indoor temperature is higher than the outdoor temperature. Because of indoor moisture production this results in a vapour pressure gradient from inside to outside. However, the relative humidity outdoors is always higher than indoors. Consequently, both gradients are opposed to each other. This leads to a net moisture flow through the considered capillary from inside to outside, as long as the material is dry. With rising water content, vapour diffusion is increasingly counterbalanced by liquid transport in the sorbate film, until the net moisture flux becomes inverse by capillary transport. In a monolithic wall, many different pores are present and depending on their dimension they favour vapour diffusion or liquid transport. It is therefore obvious that a differentiation of both moisture transport mechanisms is very important for the modelling of this phenomena, which usually occurs during the winter season. Despite the fact that an interaction of liquid and vapour fluxes, especially under very humid conditions, cannot be excluded, they are treated as independent processes in the model presented here.

2.2.1. *Vapour diffusion.* Vapour diffusion in porous media which occurs as Fick's diffusion and effusion depending on the pore size [11] (thermodiffusion is negligible in building science [3]) can be described by the following equation:

$$g_v = -\delta_p \nabla p = -\frac{\delta}{\mu} \nabla p. \tag{1}$$

The vapour diffusion resistance number μ is a constant (!) material property which accounts for the free cross-section and tortuosity of the pores, as well as the relation between the above mentioned diffusion mechanisms. It has to be determined by standard 'cup'-tests under dry conditions. The so-called wet-cup test is not appropriate because liquid transport might 'enhance' the diffusion flux.

2.2.2. *Liquid transport.* The liquid transport incorporates the liquid flow in the absorbed layer, also called surface diffusion, and in the water filled capil-

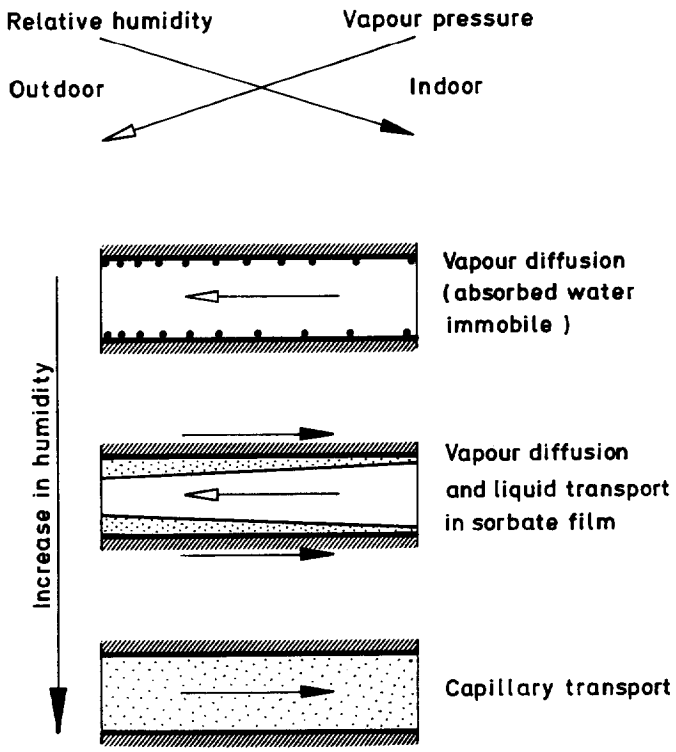

Fig. 4. Schematic representation of the driving potentials for the moisture migration in capillary pores in a monolithic wall under winter conditions.

laries (capillary transport). The driving potential is in both cases the capillary suction stress resp. the relative humidity. According to ref. [7] the liquid transport can be described by

$$g_w = -D_\varphi \nabla_\varphi. \tag{2}$$

The liquid conductivity D_φ is a function of the relative humidity. Its temperature dependence is in inverse ratio to the temperature dependence of the viscosity of water. In the hygroscopic moisture range it can be determined by wet-cup tests [7]. For higher water contents (moisture range B in Fig. 1) it has to be deduced from the liquid diffusivity D_w, which can be determined from transient moisture profile measurements, as for example described in ref. [9]. The relationship between D_φ and D_w can be expressed by

$$D_\varphi = D_w \cdot \mathrm{d}w/\mathrm{d}\varphi, \tag{3}$$

where $\mathrm{d}w/\mathrm{d}\varphi$ is the derivative of the water retention function.

The liquid diffusivities derived from moisture profiles during water absorption and after separation from the water source during the liquid redistribution process in a natural sandstone sample are plotted in Fig. 5 as a factor of the water content related to the capillary saturation w_f. Both coefficients increase considerably with water content, but there is a clear difference between the results for the absorption and the redistribution diffusivity. This can be explained by a close look at the transport phenomena in the microstructure. While the largest capillaries bear the main influx during the water absorption, they are almost inactive during the redistribution process due

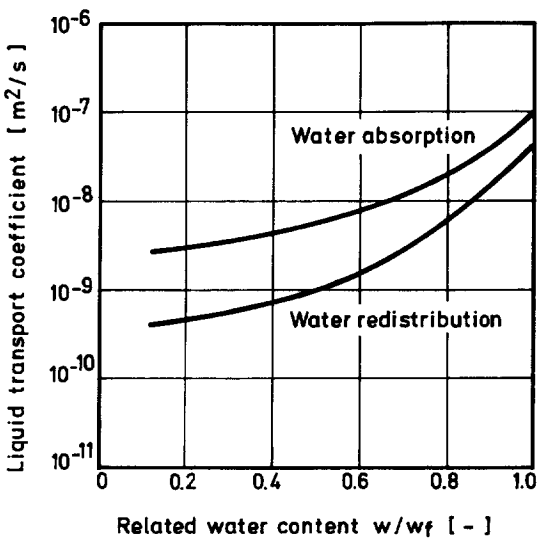

Fig. 5. Liquid diffusivities of Sander sandstone determined from transient moisture profiles recorded with an NMR-scanner during water absorption and redistribution [14].

to counterbalancing menisci which form as soon as the sample is separated from the water source. At that stage when the moisture profiles have hardly changed, only the smaller pores can extract the water from the large capillaries and thereby redistribute the water, a process which is comparatively slow. Around the equilibrium water content at 60% r.h. both functions are rapidly approaching zero, therefore the graphs in Fig. 5 stop there.

3. CALCULATION MODEL FOR THE COUPLED HEAT AND MOISTURE TRANSFER

An enquiry on calculation models in ref. [12] shows that while temperature is the only potential used for heat transfer, there is a great choice of possible potentials for moisture transport. It has been indicated in the introduction that potentials which are not physical driving forces, or which are not continuous in a multilayer building component are considered to not be appropriate for the modelling task. Of course, formulations using different potentials can be mathematically identical, but the derivation of the transport equations (1) and (2) to fit into a model, using for example water content and temperature as potentials, entails among other problems latent numerical errors, which has been demonstrated in ref. [7]. In order to facilitate plausibility checks the driving potentials should be widely known quantities which are easily measurable. All these requirements are met by the real driving forces for moisture transport, the vapour pressure and the relative humidity [see equations (1) and (2)] which will therefore be used for the following transport equations.

Disregarding vapour and liquid convection caused by total pressure differences or gravitation, as well as enthalpy changes by liquid flow which have only a negligible effect on the heat balance [7], the coupled differential equations can be expressed in terms of the independent variables temperature θ and relative humidity φ, with vapour pressure being the product of both variables

$$\left(\rho c+\frac{\partial H_w}{\partial \theta}\right)\cdot\frac{\partial \theta}{\partial t}=\nabla\cdot(\lambda\nabla\theta)+h_v\nabla\cdot(\delta_p\nabla(\varphi p_{sat})) \quad (4)$$

$$\frac{dw}{d\varphi}\cdot\frac{\partial \varphi}{\partial t}=\nabla\cdot(D_\varphi\nabla\varphi+\delta_p\nabla(\varphi p_{sat})). \quad (5)$$

On the left hand side of both equations are the storage terms. The fluxes on the right hand side are in both equations effected by heat and moisture. The conductive heat flux and the enthalpy flux by vapour diffusion with phase changes in equation (4) are strongly influenced by the moisture fields, respectively, fluxes. The liquid flux in equation (5) is only slightly influenced by the temperature effect on the liquid viscosity and consequently on D_φ. The vapour flux, however, is simultaneously governed by the temperature and moisture fields due to the exponential changes of the saturation vapour pressure with temperature. Due to this close coupling and the strong nonlinearity of both transport equations, a stable and efficient numerical solver had to be designed for their solution, which is the basis of the computer program WUFIZ described in ref. [7].

The discretization of the transport equations (4) and (5) is done by a fully implicit finite volume scheme with variable grid spacing. In the one-dimensional case this leads to difference equations which can be solved efficiently by the Thomas algorithm for tridiagonal matrices. The coupling of the discretized equations (4) and (5) is assured by iterative consecutive solution of these equations, using under relaxation factors adapted to the progress of solution. Special care must be taken in formulating the difference equations containing the vapour pressure which is a product of both transport variables. In order to avoid numerical oscillations or problems with mass conservation due to numerical inaccuracies caused by round-off errors, the derivative of vapour pressure must not be separated into derivatives of temperature and relative humidity [7].

The calculation procedure, including the necessary input and the obtainable results, are demonstrated with the aid of Fig. 6. The input data comprises:

(1) The geometry and composition of the building component, as well as the numerical grid whose spacing has to be chosen according to the expected local gradients (steep gradients in temperature and relative humidity necessitate a fine mesh for high accuracy of the results).

(2) The hygrothermal properties of the relevant building materials, i.e. dry density, porosity, heat capacity, dry thermal conductivity and its moisture dependence (usually linear relationship), dry vapour diffusion resistance number as well as water retention function and liquid diffusivities for hygroscopic, respectively, capillary active materials. If the water retention function and the liquid diffusivities are not known, approximations based on standard material properties (e.g. water absorption coefficient) can be introduced [7].

(3) The climatic indoor and outdoor boundary conditions including the appropriate time steps. As outdoor boundary conditions, hourly mean values of temperature, relative humidity, solar radiation and precipitation should be used if available (e.g. test reference years).

(4) The surface transfer or symmetry conditions at the boundaries and control parameters. The surface transfer conditions include the heat and moisture transfer coefficients, the short wave absorptivity, the long wave emissivity and the rain absorptivity of the surface (the rain absorptivity is the ratio between the amount of precipitation clinging to the surface divided by the amount hitting the surface, e.g. measured by a rain gauge). If the boundary is a symmetry plane, all transfer coefficients are equal to zero. The control

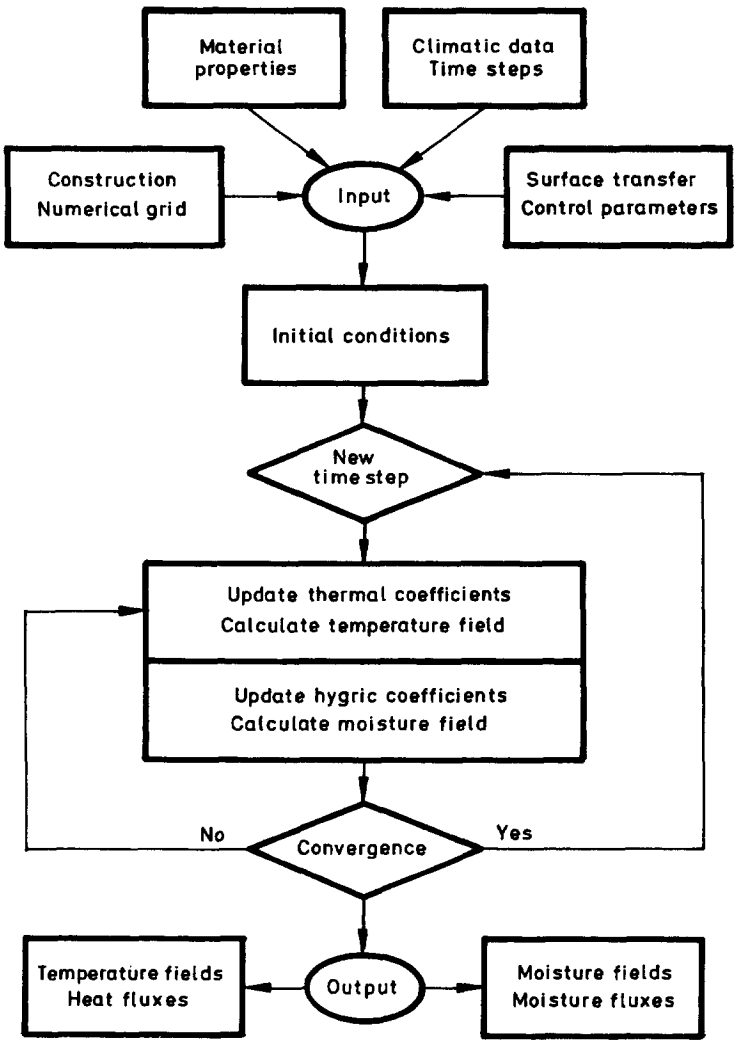

Fig. 6. Flow chart of the calculation process.

parameters permit the suppression of latent heat effects, liquid flow, etc. for comparative calculations.

After compilation of the input data the transient calculations start from initial temperature and moisture conditions, which are either based on measurements or derived from steady-state calculations, respectively, practical experience. At each time step the heat and moisture transport equations are solved consecutively with a continuous update of the transport and storage coefficients until the convergence criteria are achieved. The calculated temperature and moisture fields, as well as the heat and moisture fluxes at the surfaces of the building component, form the output data.

4. EXPERIMENTAL VERIFICATION OF THE CALCULATION RESULTS

The validation of a calculation model requires reliable experimental investigations with well documented initial and boundary conditions, as well as accurate material properties and measurement results. If these conditions are only partly met there is a danger that fitted assumptions conceal a model deficiency. The following test example of natural stone samples built in a west oriented facade was chosen because it complies with the conditions stated above.

The facade samples are 25 cm long prisms with a cross-section of 5×5 cm^2. In order to assure one-dimensional conditions the flanks were sealed and insulated before the prisms were built in the west wall of a test hall with one surface exposed to the natural climate and the other surface, which is sealed to avoid condensation, exposed to the indoor conditions. Starting from dry initial conditions, the moisture behaviour of the exposed samples was determined by pulling them out of the test wall about every second day for weighing. On a few occasions their moisture profiles were also measured with the aid of an NMR-scanner. During the whole test period the outdoor temperature

Table 1. Standard material properties of Sander sandstone

Density [kg m^{-3}]	2100
Porosity [%]	16
Heat capacity [kJ kg^{-1} K^{-1}]	0.9
Thermal conductivity [W m^{-1} K^{-1}]	1.6
Increase in thermal conductivity by moisture [% M.-% $^{-1}$]	8
Vapour diffusion resistance number	32

and humidity, the west radiation and the driving rain (rain gauge integrated in test facade) were continuously registered and recorded as hourly mean values. The standard material properties of the natural stone, a sandstone from the Main region, are listed in Table 1. The water retention function and the liquid diffusivities have already been shown in Figs. 3 and 5. When rain water hits the sample surface the calculation for that particular time step is carried out taking the liquid diffusivity for water absorption, otherwise the diffusivity for liquid redistribution is chosen. The short wave absorptivity lies between 0.7 for dry and 0.85 for wet surface conditions. Thus all required input data for the calculation have been measured, except for the surface transfer coefficients and the rain absorptivity, which have to be taken from literature or experience. The heat transfer coefficients are assumed to be 8 W m^{-2} K^{-1} indoors and 17 W m^{-2} K^{-1} outdoors [13]. The resulting outdoor vapour transfer coefficient is $7.5 \cdot 10^{-8}$ kg m^{-2} s^{-1} Pa^{-1} and the choice of the rain absorptivity is 0.7.

The results for the total moisture in the facade samples over a period of 80 days starting from the beginning of September is compared with the calculation results in Fig. 7, at the bottom. Above, the outdoor climate conditions are plotted as daily mean or sum (the calculations were carried out with hourly values). The indoor temperature of the unheated test hall decreased quite steadily from 21 to 10°C during the considered period. The moisture profiles recorded at four different time points in the observation period are plotted together with the calculated profiles in Fig. 8. The comparisons in Figs. 7 and 8 show an almost perfect agreement between the measured and the calculated results for the course of total moisture and the moisture profiles in the natural stone facade samples.

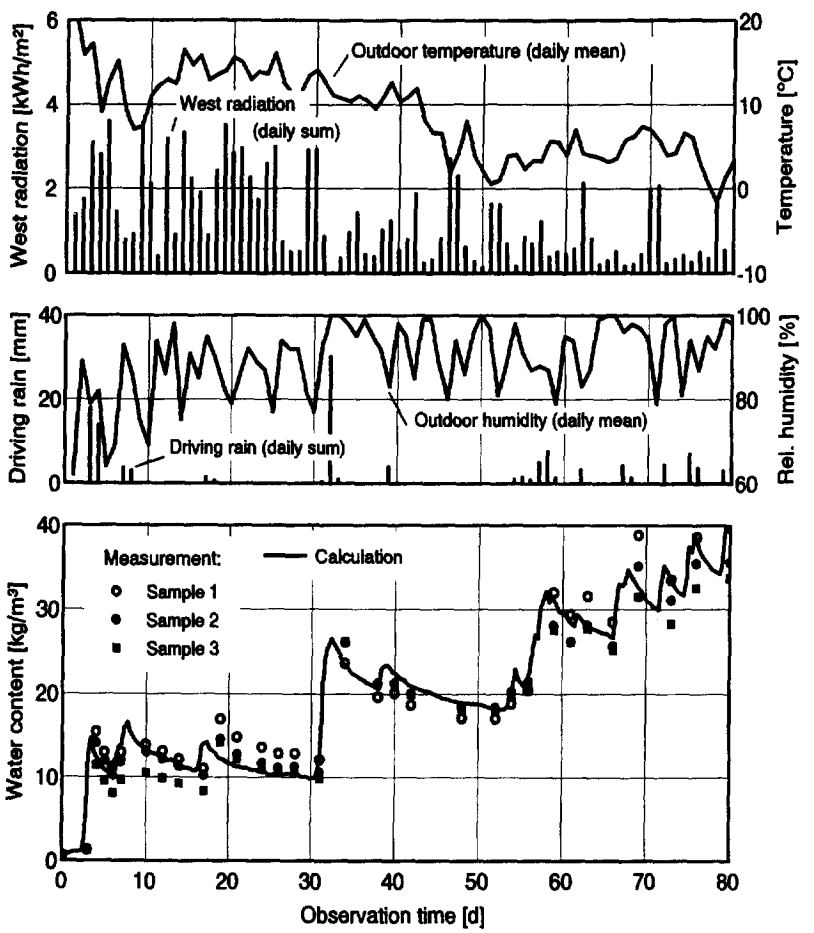

Fig. 7. Calculated course of the mean water content in a 25 cm thick natural stone facade in comparison to measured results from three exposed facade samples including climatic conditions.

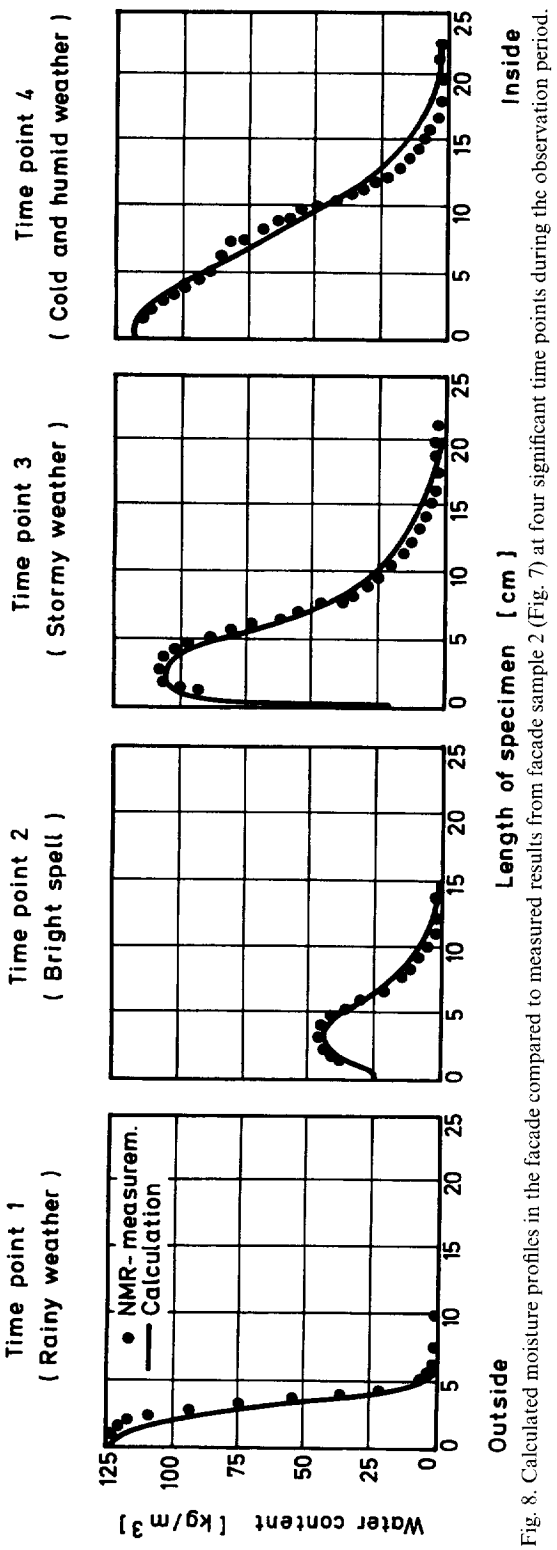

Fig. 8. Calculated moisture profiles in the facade compared to measured results from facade sample 2 (Fig. 7) at four significant time points during the observation period.

5. CONCLUSIONS

Together with two other test examples in ref. [7], of which one is a two-dimensional application, the experimental verification of the calculation results shows the validity of the model. Because the required material properties are comparatively simple and easy to determine, a greater variety of building materials can be examined than in the past when cellular concrete was the favourite guinea pig. The choice of the well known quantities temperature and relative humidity as potentials and transported variables facilitates the definition of the boundary conditions, and the plausibility checks of the calculation results. Therefore a more wide spread application of heat and moisture transfer calculations in building science can be expected in the future.

However, it should be pointed out that even the best model cannot replace the real field test, because in practice there are always some effects not considered in the model which might be of predominant importance. Therefore, a model like the one presented here can only supplement the field test, for example by extrapolating the results or assessing the influence of different climate conditions. Without experimental verification, the calculation results can only show a trend or estimate the importance of certain hygrothermal effects.

Acknowledgement—The authors thank the German Ministry for Research and Technology and industrial contract partners who funded this work in the frame of a monument conservation project and the project Annex 24 of the International Energy Agency (IEA). It should be mentioned that the co-operation of scientists from 14 countries during Annex 24 contributed considerably to accomplishing the task.

REFERENCES

1. A. V. Luikov, Systems of differential equations of heat and mass transfer in capillary-porous bodies, *Int. J. Heat Mass Transfer* **18**, 1–14 (1975).
2. J. R. Philip and D. A. de Vries, Moisture movement in porous materials under temperature gradients, *Trans. Am. Geophys. Union* **2**, 222–232 (1957).
3. K. Kießl, Kapillarer und dampfförmiger Feuchtetransport in mehrschichtigen Bauteilen, PhD-thesis, University of Essen, Essen (1983).
4. C. R. Pedersen, Combined heat and moisture transfer in building constructions, PhD-thesis, Technical University of Denmark, Lyngby (1990).
5. J. Neiß, *Numerische Simulation des Wärme- und Feuchtetransport und der Eisbildung in Böden*. VDI, Düsseldorf (1982).
6. M. Matsumoto and M. Sato, A harmonic analysis of periodic steady state solution of the internal condensation process, *Proceedings CIB W 67-Symposium*, Vol. 2, Rotterdam (1990).
7. H. M. Künzel, *Simultaneous Heat and Moisture Transport in Building Components*. IRB, Stuttgart (1995).
8. M. Krus and K. Kießl, Vergleichende Untersuchungen zur Bestimmung der Porenradienverteilung von Natursandsteinen mittels Saugspannungsmessung und Quecksilber-Druckporosimetrie, Fraunhofer-Institut für Bauphysik, report FtB-11/1991.
9. K. Kießl, M. Krus and H. M. Künzel, Weiterentwickelte

Meß- und Rechenansätze zur Feuchtebeurteilung von Bauteilen. Praktische Anwendungsbeispiele, *Bauphysik* **15**, 61–67 (1993).
10. DIN 4108, Teil 5, Wärmeschulz im Hochbau; Berechnungsverfahren, August (1981).
11. K. Gertis, Hygrische Transportphänomene in Baustoffen. In: *Schriftenreihe des Deutschen Ausschuß für Stahlbeton*, Vol. 258. Ernst and Sohn, Berlin (1976).
12. H. Hens and A. Janssens, Enquiry on HAMCaT Codes, IEA-Annex-24 interim's report, Katholic University of Leuven, Belgium (1992).
13. H. Schaube and H. Werner, Wärmeübergangskoeffizient unter natürlichen Klimabedingungen, IBP-Mitteilung no. 109 (1986).
14. M. Krus, *Moisture Transport and Storage Coefficients of Porous Building Materials*. IRB, Stuttgart (1996).